PROCEEDINGS OF SCIENCE

Diffuse Emission of Galactic High-Energy Gamma-Rays and Neutrinos from a Global Fit of Cosmic Rays

Georg Schwefer,[a,b,c,*] **Philipp Mertsch**[a] **and Christopher Wiebusch**[b]

[a] *Institute for Theoretical Particle Physics and Cosmology (TTK), RWTH Aachen University, 52056 Aachen, Germany*

[b] *III. Physikalisches Institut B, RWTH Aachen University, 52056 Aachen, Germany*

[c] *Max-Planck-Institut für Kernphysik, Saupfercheckweg 1, 69117 Heidelberg, Germany*

E-mail: georg.schwefer@mpi-hd.mpg.de, pmertsch@physik.rwth-aachen.de, wiebusch@physik.rwth-aachen.de

In the standard picture of galactic cosmic rays, a diffuse flux of high-energy gamma-rays and neutrinos is produced from inelastic collisions of cosmic ray nuclei with the interstellar gas. The neutrino flux is a guaranteed signal for high-energy neutrino observatories such as IceCube, and first evidence was recently found. In gamma-rays, the LHAASO experiment also recently reported on the measurement of diffuse gamma-rays up to 1 PeV in energy. The measurements of these fluxes constitute an important test of the standard picture of galactic cosmic rays. Both the observation and non- observation allow important implications for the physics of cosmic ray acceleration and transport. We present `CRINGE`, a new model of galactic diffuse high-energy gamma-rays and neutrinos, based on a cosmic ray model that is obtained from a fit to data from AMS-02, DAMPE, IceTop as well as KASCADE. We discuss the uncertainties for the predicted emission from the cosmic ray model, but also from the choice of source distribution, gas maps and cross sections and consider the possibility of a contribution from unresolved sources. We find the overall uncertainty on the emission to vary between 10% and 30% at energies below 10 TeV and up to 50% above, with the uncertainty from the fit to CR data dominating in this energy range. The contribution from unresolved sources can potentially be of the same order of magnitude as the truly diffuse flux and can lead to significantly harder spectra. We compare the prediction of the `CRINGE` model with the recent data from LHAASO and IceCube and comment on the implications. Our fiducial model and cosmic ray spectra are publicly available on zenodo.

38th International Cosmic Ray Conference (ICRC2023)
26 July - 3 August, 2023
Nagoya, Japan

*Speaker

PoS(ICRC2023)1502

1. Introduction

The galactic diffuse emission (GDE) of both gamma-rays and neutrinos from the Milky Way stems from interactions of galactic cosmic rays (GCRs) with the interstellar gas and radiation fields. It therefore offers unique insights into the spatial and spectral distribution of GCRs in the galaxy [1] and thus towards answering the question of the origin and propagation of GCRs. In a recent work [2], we presented the `CRINGE`[1] model of GDE based on a global fit to recent data on local GCR fluxes. The uncertainties from the GCR model parameters and the further GDE inputs are also assessed in this model's framework, as are unresolved sources through the model from [3]. Since then, new measurements of the very high-energy diffuse gamma-ray emission from the LHAASO experiment [4] as well as the first reported evidence for galactic neutrino emission from the IceCube collaboration [5] have become available. Here, after a summary of the methodology of the `CRINGE` model, we compare these new results to the `CRINGE` model and discuss their implications.

2. Method

In this section, we briefly recap the methodology of the `CRINGE` model, paraphrasing [2, Sec. 2]. For a more extensive description we refer the reader to [2]. Building a model of diffuse gamma-rays and neutrinos requires three main inputs: a model for the distribution of GCRs, a map of the interstellar gas and radiation field (ISRF) in the Milky Way, and the hadronic production cross sections. We provide an explanation of the choices made for the CRINGE model for each of these and detail the global fit to GCR data to determine the parameters of our GCR model.

2.1 Galactic Cosmic Ray Model

We model the propagation of GCRs with a pure diffusion model. We assume an axisymmetric galaxy with a half-height $z_{\mathrm{max}} = 6\,\mathrm{kpc}$ and radius $r_{\mathrm{max}} = 20\,\mathrm{kpc}$. The diffusion coefficient, $D(\mathcal{R})$, is taken to be homogeneous and isotropic with a four-times broken power law rigidity dependence. The four spectral breaks are introduced to model the softenings in gamma-ray spectra of supernova remnants observed by *Fermi*-LAT [e.g. 6] similar to what was done in [7], the breaks around 300 GV and 10 TV observed by direct cosmic ray measurements [e.g. 8, 9] and finally the well-known cosmic ray "knee" around ~ PV. The strengths of the spectral breaks, their precise rigidities and the overall normalization of the diffusion coefficient are free fit parameters.

For the GCR source injection, we factorize into a spatial source distribution $S(r, z)$ and an injection spectrum, $g(p)$. The spatial structure of the model's predicted emission is heavily influenced by the assumption made for $S(r, z)$. We take this uncertainty into account by using four different, well-established distributions [10–13]. The injection spectra $g(p)$ for all nuclei are modelled as single power laws, with the spectral indices allowed to vary between different species. Our model for the injection of leptons follows [7],where electrons are assumed to be injected with a twice broken power law spectrum with a high-energy cutoff and the spectral hardening in the positron spectrum at GeV energies [14] is treated through an extra source component. A once broken power law with an exponential cut-off is assumed as its injection spectrum.

[1] **C**osmic **R**ay-fitted **In**tensities of **G**alactic **E**mission

2.2 Interstellar Medium Components

Atomic hydrogen (HI) maps can be obtained from surveys of the 21 cm emission line from the hyperfine transition [15, 16]. Converting the measured line brightness to gas column density requires the assumption of a spin temperature T_s, equivalent to an optical depth of the line. We here use three different models of the gas distribution for an assessement of the corresponding uncertainty. The first is the `GALPROP` model, which makes use of the LAB HI survey data [15] and has $T_s = 150$ K. The second model, called `GALPROP-OT`, only differs from the `GALPROP` model in assuming the gas to be optically thin with $T_s = 10^5$ K. Lastly, the `HERMES` model is based on data from the HI4PI HI survey [16] and has $T_S = 300$ K [17].

Our assumed model of molecular hydrogen (H_2) is based on the data from the CfA carbon monoxide $J = 1 \rightarrow 0$ line emission survey compilation from [18]. To convert the measured line intensity to gas column density, a phenomenological conversion factor $X_{\rm CO}$ is used. We take this factor to be a constant throughout the galaxy with a value of $X_{CO} = 2 \times 10^{20}$ cm^{-2} (K km s^{-1})$^{-1}$.

Finally, we employ two different models of the ISRF, namely those from [19] (henceforth called `GALPROP`) and [20]. These differ in their calculation of the accumulated starlight in the Milky Way and its reprocessing in interstellar dust, the former using a numerical approach, the latter an analytical one, and give quantitatively different results.

2.3 Hadronic Production Cross Sections

Hadronic gamma-ray and neutrino production cross sections, calculated assuming different hadronic interaction models, represent a major uncertainty in the modelling of GDE [e.g. 21]. To quantitatively assess this, we use the following three models: The first of these (here called K&K) is a combination of the total inelastic p-p cross section from [22] with the secondary yields and spectra from [23]. In the second model, the parameterization from [24] is taken for primary energies below 500 TeV and the K&K model is used at higher energies. The last model is the `AAfrag` model described in [21].

2.4 Unresolved Sources

To model the flux of unresolved sources at TeV energies, we follow [3]. Their model is based on a model of the population of pulsar-powered sources as seen by gamma-ray observations at TeV energies. Leaving open the possibility that the gamma-ray emission is of hadronic origin, we also consider the neutrino flux from the same sources as an addition to the diffuse neutrino flux.

2.5 Gamma-Ray Absorption

We treat the absorption of gamma-rays above a few TeV in a simplified manner, and, following App. E of [25] [2], calculate an absorption probability $p_{\rm abs}(E, \Omega)$. With this, the absorbed gamma-ray intensity, $J_{\rm abs}(E, \Omega)$ is related to the non-absorbed intensity J as $J_{\rm abs}(E, \Omega) = p_{\rm abs}(E, \Omega) J(E, \Omega)$

2.6 Global Fit

Overall, 26 parameters in our model of GCRs (see [2, Tab. 1]) are fitted to local measurements of GCR intensities. Eight further fit parameters also listed in [2, Tab. 1] are necessary in the procedure

[2] We are grateful to to Mischa Breuhaus for providing his calculation, which makes use of the GAMERA code [26].

of the fit. These are four solar modulation potentials [27] and four energy-scale parameters. The latter four rescale the measured hadronic GCR intensities following [28] and are required to mitigate inconsistencies between experiments. The data we fit to comes from direct measurements by AMS-02 (p [8], He [29], C [29], e^- [30], e^+ [14] and B/C [31]) and DAMPE (p [8] and He [32]) as well as indirect measurements of protons and helium from IceTop [33] and KASCADE [34] based on the SIBYLL-2.1 interaction model. To calculate the distribution of GCRs from our model, we have used the `DRAGON` code [35] modified to handle our model for the diffusion coefficient. The resulting hadronic GDE is then calculated with the `HERMES` code [36], featuring our implementation of the `GALPROP`(-OT) gas maps as well as the `AAfrag` cross section on top of the public version.

As the statistical model for our fit, we take a Gaussian likelihood function. To find the best fit values and the uncertainties of the parameters, we use an MCMC sampling method. For our application, the benefits of this method - its robustness against getting stuck in local minima in a high-dimensional parameter space and the immediate output of parameter uncertainties through the credible intervals - clearly outweigh its main drawback, the long computation times.

3. Results

3.1 Galactic Cosmic Ray Intensities

In figure 1 we show the resulting intensities of proton and helium from our fit together with the energy-rescaled data used in the fit[3]. Overall, the GCR data is adequately described by our best-fit model (black line). The χ^2 values for the individual observables can be found in [2, Tab. 2]. The widths of the 68 % and 95 % uncertainty bands reflect the constrains imposed by the data. In particular, when only indirect observations constrain the model, the uncertainty grows significantly. This is exacerbated by the residual discrepancies between IceTop and KASCADE data, which are present inspite of the energy-rescaling. In consequence, this is the most important source of uncertainty in the GCR model.

3.2 Diffuse Gamma-Ray Intensities

Our fiducial model is calculated with the source distribution from [10], the `GALPROP` galactic gas maps and ISRF as well as the `AAfrag` production cross sections as input models. The uncertainty from the fit to GCR data is taken to be the central 68 % interval of the posterior distribution of GDE intensities. The other uncertainties are separately calculated for each input by recomputing the GDE with each member of the set of different choices for that input as listed in section 2, and taking the standard deviation of the resulting intensities. In this, the GCR parameters are always fixed to their best-fit values. In figures 2 and 3, these uncertainties are displayed as uncertainty bands. In figure 2, we compare the prediction of the `CRINGE` model with and without unresolved sources to the recent LHAASO results [4] in both the inner ($|b| < 5°$,$15° < l < 125°$) and outer ($|b| < 5°$,$125° < l < 235°$) window. To account for the mask applied in the analysis of the LHAASO data, we multiply the LHAASO points by factors of 1.61 (inner window) and 1.02 (outer window) respectively. These factors are calculated in [4] under the assumption of a spatial template proportional to the *Planck* dust opacity maps, which is essentially equivalent to the assumption of

[3]For the results of the fit to the other GCR species, see [2, Fig. 5]

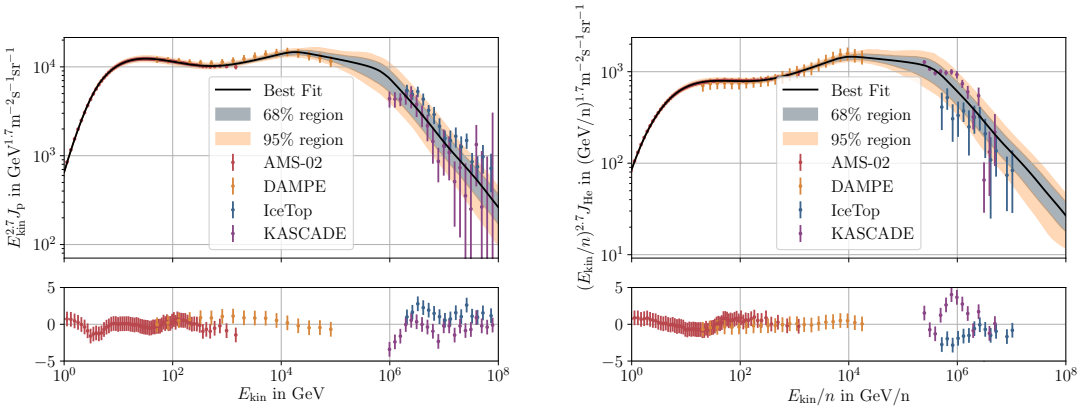

Figure 1: Model spectra for GCR protons (left) and helium (right) together with the data used in the fit. The best fit model (solid black line) and the 68 % and 95 % uncertainty intervals (gray and light orange bands) are displayed in the upper panel together with the observations by AMS-02 [8, 14, 29–31], DAMPE [9, 32], IceTop [33] and KASCACE [34]. The lower panels show pull plots.

a spatially uniform GCR density. In reality, however, the GCR density is very likely to increase towards the galactic center [1]. Together with the fact that in the inner window, the fraction of the analysis region that is masked out increases towards the galactic center, this means that the correction in the inner window as given in [4] can really be seen as a lower bound. In the outer window, because of the smaller masked area and the smaller gradient in the GCR density profile, this effect is not nearly as relevant. In the inner window, we find the LHAASO measurement to lie above the prediction of the `CRINGE` model when only considering truly diffuse emission. The measurement in this area is however consistent with the prediction when the contribution from unresolved sources is added. In this case, the measurement lies towards the lower end of the uncertainty band of the predicted flux. In the outer window, we find a very similar picture. Note that in this window, the LHAASO measurement is also consistent with the truly diffuse flux, if its true value lies at the very upper end of the given uncertainty range.

3.3 Diffuse Neutrino Intensities

To compare the `CRINGE` model to the recent IceCube results [5], we limit ourselves to a window around the galactic center ($|b| < 8°$,$|l| < 8°$). This is because this region has by far the largest contribution to the test statistic determined in the IceCube analysis [5, Fig. 3] and is therefore the region its result is mainly derived from. The IceCube results are simply scalings of the Fermi-π^0 [37], KRAγ-5 [38] and KRAγ-50 [38] models. Note that in the IceCube fit, the spectral index of the energy spectrum is averaged over the spatial template for the KRAγ models. The baseline values of these models are also shown in figure 3. The figure shows that above 10 TeV, the IceCube measurements exceed the prediction of the `CRINGE` model when only truly diffuse emission is considered. At lower energies, the conclusions depend on the model tested by the IceCube analysis. For the KRAγ models, there is agreement between the `CRINGE` prediction and the measurements, whereas the result derived with the Fermi-π^0 model still exceeds the `CRINGE` prediction by a factor of 2-3. As a consequence, when adding the model of unresolved sources from [3], one finds that

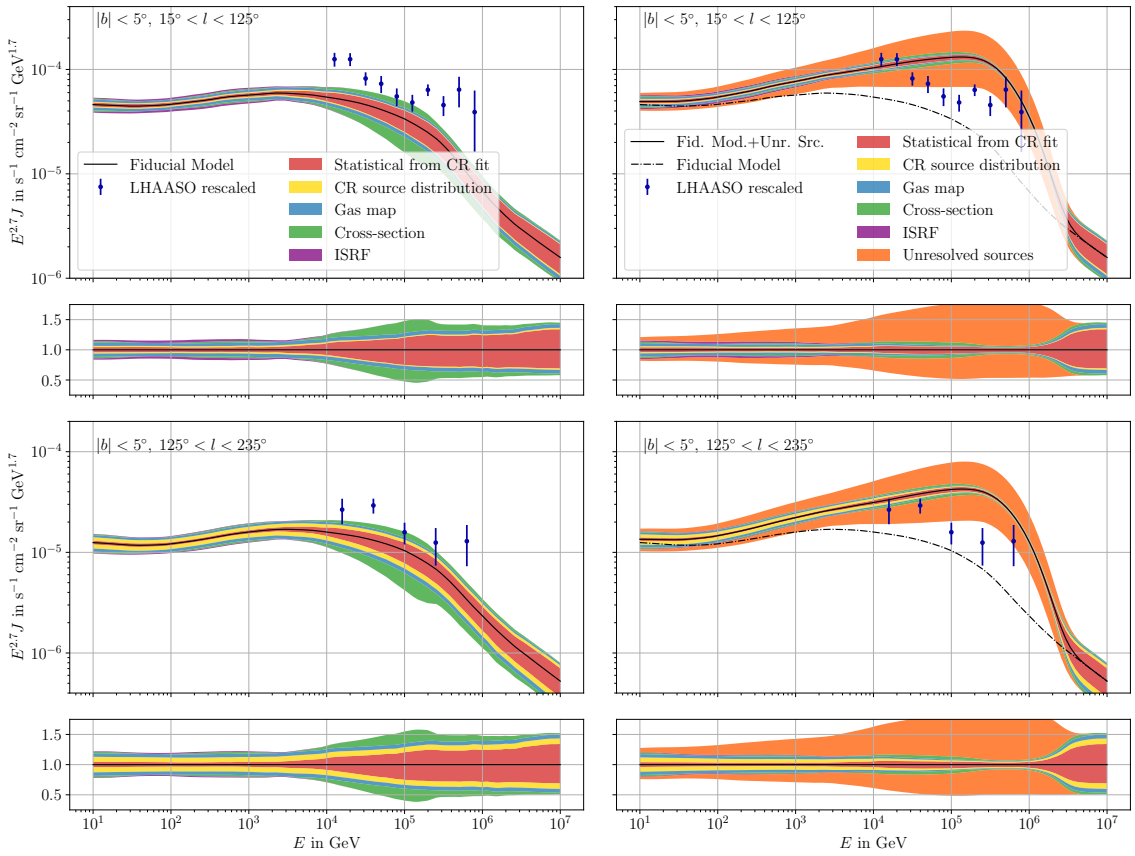

Figure 2: Gamma-ray intensity spectra in two windows in the galactic plane: $|b| < 5°$, $15° < l < 125°$ (*inner*, top row) and $|b| < 5°$, $125° < l < 235°$ (*outer*, bottom row). The left column shows the prediction of our fiducial model of truly diffuse emission only, the right column show the prediction combined with the model of unresolved sources from [3]. The shaded bands represent the uncertainties from the various inputs to the GDE model, the magnitude of which relative to the prediction of the fiducial model can be seen in the lower panels. The model is compared with the observations by LHAASO [4], rescaled by factors of 1.61 (inner) and 1.02 (outer), respectively, to correct for the applied source mask as suggested in [4].

the IceCube result derived with the Fermi-π^0 model is very consistent with the prediction, whereas the results derived with the KRAγ models drop below the prediction below 10 TeV.

4. Discussion and Conclusions

The comparison of the `CRINGE` model with the measurements in figures 2 and 3 shows that an additional flux of unresolved sources on top of the truly diffuse emission is likely necessary to match the measurements, a conclusion also recently drawn in [e.g. 39]. Note that on the basis of this alone, other scenarios leading to GDE intensities greater than predicted by the `CRINGE` model such as those presented in [40] can of course not be excluded. A corollary of this is that scenarios for the transport of GCRs at TeV and PeV energies that would lead to lower GDE intensities than the homogeneous and isotropic diffusion assumed for the `CRINGE` model are only viable when a very large contribution from unresolved sources is considered.

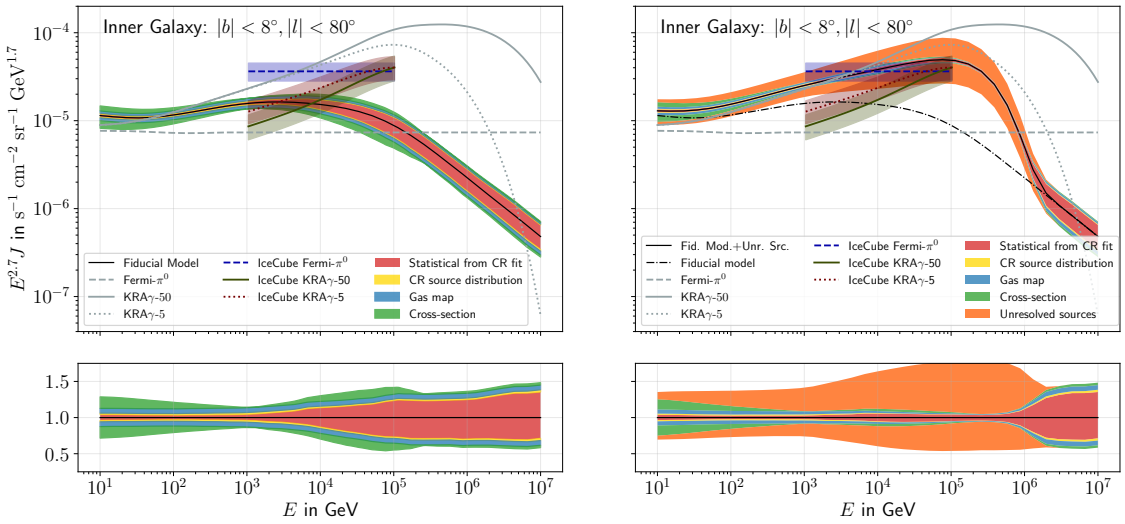

Figure 3: Neutrino intensity spectra in the window $|b| < 8°$, $|l| < 80°$. The left column shows the prediction of our fiducial model of truly diffuse emission only, the right column show the prediction combined with the model of unresolved sources from [3]. The shaded bands represent the uncertainties from the various inputs to the GDE model, the magnitude of which relative to the prediction of the fiducial model can be seen in the lower panels. The baseline intensities predicted by the Fermi-π^0, KRAγ-5, and KRAγ-50 models are shown in the dashed, dotted and solid gray lines, respectively. The IceCube measurements reported in [5] along with their uncertainties are indicated by the shaded bands around the blue, green and red lines.

Regarding the morphology of GDE, we note that the LHAASO measurements exceed the prediction of our fiducial model by a similar factor 2 in both windows. This is an indication that the morphology of the additional flux component needed to explain the measurements does not strongly deviate from the morphology of the truly diffuse emission determined by the product of GCR and gas distributions in the Milky Way. The morphology resulting from the model of unresolved sources considered in this work appears similar enough to give a consistent description in both windows. The conclusions drawn on this matter from the IceCube measurements somewhat depend on the particular model considered in the analysis. However, above 10 TeV, i.e. the range that overlaps with the LHAASO measurements, the excess is at a similar level as seen there, strengthening the above conclusions. This similarity is also a clear indicator that the observed GDE of gamma-rays is primarily produced in hadronic processes. Measurements in different channels in IceCube such as [41], which also sees an excess of neutrinos from the galactic plane, but is sensitive in a different region of the plane, will help shed further light on this issue.

On the energy spectrum of the GDE, we remark on the consistency between the spectra measured by LHAASO in both windows, which challenge models with a spectrum dependent on galactocentric radius such as the KRAγ models and those shown in [40]. Beyond this, it is also noteworthy that the LHAASO result shows no signs of a spectral softening above 100 TeV that would reflect the cosmic ray "knee". This will be interesting to monitor while the measurements of GDE will inevitably become more precise over the next few years.

Finally, we reiterate that our fiducial gamma-ray and neutrino models, the underlying GCR distributions and the fitted local GCR fluxes with their uncertainties are available on zenodo.

References

[1] L. Tibaldo, D. Gaggero and P. Martin *Universe* **7** (2021) 141 [2103.16423].
[2] G. Schwefer, P. Mertsch and C. Wiebusch ApJ **949** (2023) 16 [2211.15607].
[3] V. Vecchiotti et al. ApJ **928** (2022) 19 [2107.14584].
[4] LHAASO collaboration 2305.05372.
[5] IceCube collaboration *Science* **380** (2023) 1338.
[6] Fermi-LAT collaboration ApJ **706** (2009) L1 [0910.0908].
[7] A. Vittino et al. Phys. Rev. D **100** (2019) 043007 [1904.05899].
[8] AMS collaboration Phys. Rev. Lett. **114** (2015) 171103.
[9] DAMPE collaboration *Sci. Adv.* **5** (2019) [1909.12860].
[10] K. Ferrière *Reviews of Modern Physics* **73** (2001) 1031 [astro-ph/0106359].
[11] G.L. Case and D. Bhattacharya ApJ **504** (1998) 761 [astro-ph/9807162].
[12] D.R. Lorimer et al. MNRAS **372** (2006) 777 [astro-ph/0607640].
[13] I. Yusifov and I. Kücük A&A **422** (2004) 545 [astro-ph/0405559].
[14] AMS collaboration Phys. Rev. Lett. **122** (2019) 041102.
[15] P.M. Kalberla et al. A&A **440** (2005) 775 [astro-ph/0504140].
[16] N. Ben Bekhti et al. A&A **594** (2016) [1610.06175].
[17] Fermi-LAT collaboration ApJS **223** (2016) 26 [1602.07246].
[18] T.M. Dame, D. Hartmann and P. Thaddeus ApJ **547** (2001) 792 [astro-ph/0009217].
[19] T.A. Porter et al. ApJ **682** (2008) 400 [0804.1774].
[20] S. Vernetto and P. Lipari Phys. Rev. D **94** (2016) 063009 [1608.01587v2].
[21] S. Koldobskiy et al. Phys. Rev. D **104** (2021) 123027 [2110.00496].
[22] E. Kafexhiu et al. Phys. Rev. D **90** (2014) 123014 [1406.7369].
[23] S.R. Kelner, F. Aharonian and V.V. Bugayov Phys. Rev. D **74** (2006) [astro-ph/0606058].
[24] T. Kamae et al. ApJ **647** (2006) 692 [astro-ph/0605581].
[25] M. Breuhaus et al. A&A **661** (2022) [2201.03984].
[26] J. Hahn *PoS* **ICRC2015** (2016) 917.
[27] L.J. Gleeson and W.I. Axford ApJ **154** (1968) 1011.
[28] H.P. Dembinski et al. *PoS* **ICRC2017** (2018) 533 [1711.11432].
[29] AMS collaboration *Phys. Rev. Lett.* **119** (2017) 251101.
[30] AMS collaboration Phys. Rev. Lett. **122** (2019) 101101.
[31] AMS collaboration *Phys. Rev. Lett.* **120** (2018) 021101.
[32] DAMPE collaboration Phys. Rev. Lett. **126** (2021) 201102 [2105.09073].
[33] IceCube collaboration Phys. Rev. D **100** (2019) 082002 [1906.04317].
[34] KASCADE collaboration *Astropart. Phys.* **24** (2005) 1 [astro-ph/0505413].
[35] C. Evoli et al. J. Cosmology Astropart. Phys. **10** (2008) 018 [0807.4730].
[36] A. Dundovic et al. A&A **653** (2021) [2105.13165].
[37] Fermi-LAT collaboration ApJ **750** (2012) 3 [1202.4039].
[38] D. Gaggero et al. Phys. Rev. D **91** (2015) 083012 [1411.7623].
[39] C. Shao, S. Lin and L. Yang 2307.01038.
[40] P. de la Torre Luque et al. 2203.15759.
[41] IceCube collaboration ApJ **849** (2017) 67 [1707.03416].